Synthesis of Mesoporous Carbon Foams Templated by Organic Colloids

Wayne W. Lukens† and Galen D. Stucky*

Department of Chemistry and Materials Research Laboratory, University of California, Santa Barbara, Santa Barbara, California 93106

Received September 21, 2001. Revised Manuscript Received December 31, 2001

Resorcinol/formaldehyde (RF) sols have useful similarities to silica sols in that both are anionic at high pH and capable of hydrogen bonding at low pH. These similarities can be exploited to prepare composite materials analogously to the synthesis of siliceous mesocellular foams (Si-MCFs). Microemulsion-polymerized polystyrene (PS) microspheres were used as templates to produce composite materials with RF polymer. Upon pyrolysis under argon, these PS/RF composites yielded mesoporous carbon foams (C-MCFs) in which the pore size was roughly two-thirds that of the template. Syntheses without the template did not produce mesoporous materials. These C-MCFs can be synthesized quickly and have properties similar to those of carbon aerogels with the same density.

Introduction

Synthesis of mesoporous carbon materials using inorganic templates is currently an active area of research due, in part, to the properties of mesoporous carbon, which include high specific surface area, high pore volume, and good electrical conductivity.[1−7] These properties have been well studied in the prototypical mesoporous carbon material, carbonized resorcinol/formaldehyde (RF) aerogel (carbon aerogel),[8,9] which has applications that include use in double-layer capacitors and capacitive deionization.[10−13]

A major difference between carbon aerogel and the templated materials is the origin of the pores. In templated mesoporous materials, well-defined pores are created by dissolving the template, generally silica, using either hydrofluoric acid or concentrated alkali. In carbon aerogel, the pores result from the supercritical extraction of the liquid phase of a gel network. In either case, pore formation adds an additional step to the synthesis of these materials. This step could be eliminated if the pores were formed using a template that would depolymerize during carbonization.

Generation of mesopores by pyrolysis of an organic component has previously been demonstrated using phase-separated polymer blends of polyethylene gycol (PEG) and polyimide[14] or poly(furfuryl alcohol).[15] In these syntheses, the pyrolysis of PEG produces mesopores in the resulting carbon material. This synthetic approach has been used introduce mesoporosity into microporous carbon materials[15] and to produce mesoporous carbon membranes.[14]

A potential route to the synthesis of a mesoporous carbon using depolymerizable organic template is suggested by the chemistries of mesoporous silica and RF. In the syntheses of templated mesoporous silica, such as MCM-41 or SBA-3, the interaction between the template and the silica sol is responsible for organizing the inorganic phase.[16] This interaction can exist between a cationic template, such as an alkylammonium group, and an anionic silicate species, as in MCM-41.[17] Alternatively, this interaction can be hydrogen bonding between the template and the silanol groups of the silica sol, as occurs during the synthesis of MSU-*X*, SBA-3, or SBA-15.[18−20] In comparison to silica sols, RF sols are

* Address correspondence to this author at Department of Chemistry, University of California, Santa Barbara, CA 93106. E-mail: stucky@chem.ucsb.edu.

† Current address: MS 70A-1150, Lawrence Berkeley National Laboratory, Berkeley, CA 94720.

(1) Johnson, S. A.; Brigham, E. S.; Ollivier, P. J.; Mallouk, T. E. *Chem. Mater.* **1997**, *9*, 2448.
(2) Han, S. J.; Sohn, K.; Hyeon, T. *Chem. Mater.* **2000**, *12*, 3337.
(3) Kawashima, D.; Aihara, T.; Kobayashi, Y.; Kyotani, T.; Tomita, A. *Chem. Mater.* **2000**, *12*, 3397.
(4) Kruk, M.; Jaroniec, M.; Ryoo, R.; Joo, S. H. *J. Phys. Chem. B* **2000**, *104*, 7960.
(5) Ryoo, R.; Joo, S. H.; Jun, S. *J. Phys. Chem. B* **1999**, *103*, 7743.
(6) Lee, J.; Yoon, S.; Hyeon, T.; Oh, S. M.; Kim, K. B. *Chem. Commun.* **1999**, 2177.
(7) Kyotani, T.; Nagai, T.; Inoue, S.; Tomita, A. *Chem. Mater.* **1997**, *9*, 609.
(8) Pekala, R. W.; Alviso, C. T. *Mater. Res. Soc. Symp.* **1999**, *270*, 3.
(9) Pekala, R. W.; Alviso, C. T.; Kong, F. M.; Hulsey, S. S. *J. Non-Cryst. Solids* **1992**, *145*, 90.
(10) Saliger, R.; Fischer, U.; Herta, C.; Fricke, J. *J. Non-Cryst. Solids* **1998**, *225*, 81.
(11) Pekala, R. W.; Farmer, J. C.; Alviso, C. T.; Tran, T. D.; Mayer, S. T.; Miller, J. M.; Dunn, B. *J. Non-Cryst. Solids* **1998**, *225*, 74.
(12) Miller, J. M.; Dunn, B.; Tran, T. D.; Pekala, R. W. *J. Electrochem. Soc.* **1997**, *144*, L309.
(13) Farmer, J. C.; Fix, D. V.; Mack, G. V.; Pekala, R. W.; Poco, J. F. *J. Electrochem. Soc.* **1996**, *143*, 159.
(14) Hatori, H.; Kobayashi, T.; Hanzawa, Y.; Yamada, Y.; Limura, Y.; Kimura, T.; Shiraishi, M. *J. Appl. Polym. Sci.* **2001**, *79*, 836.
(15) Lafyatis, D. S.; Tung, J.; Foley, H. C. *Ind. Eng. Chem. Res.* **1991**, *30*, 865.
(16) Huo, Q. S.; Margolese, D. I.; Ciesla, U.; Demuth, D. G.; Feng, P. Y.; Gier, T. E.; Sieger, P.; Firouzi, A.; Chmelka, B. F.; Schuth, F.; Stucky, G. D. *Chem. Mater.* **1994**, *6*, 1176.
(17) Kresge, C. T.; Leonowicz, M. E.; Roth, W. J.; Vartuli, J. C.; Beck, J. S. *Nature* **1992**, *359*, 710.
(18) Bagshaw, S. A.; Prouzet, E.; Pinnavaia, T. J. *Science* **1995**, *269*, 1242.
(19) Huo, Q. S.; Margolese, D. I.; Stucky, G. D. *Chem. Mater.* **1996**, *8*, 1147−1160.
(20) Zhao, D. Y.; Feng, J. L.; Huo, Q. S.; Melosh, N.; Fredrickson, G. H.; Chmelka, B. F.; Stucky, G. D. *Science* **1998**, *279*, 548.

10.1021/cm010904z CCC: $22.00
Published on Web 03/06/2002

particularly interesting because they exhibit useful similarities. Like silica sols, RF sol is anionic at high pH and capable of hydrogen bonding at low pH, because of the phenolic functional group of resorcinol. For this reason, the substitution of RF sol for silica sol seemed likely to produce a polymeric composite material that could yield mesoporous carbon upon pyrolysis.

Distinct differences, however, exist between silica sols and RF sols, most notably the fact that the siloxane bonds in silica are easily broken and reformed during synthesis whereas the carbon−carbon bonds in RF sol are not. Therefore, the structure of the resulting material might not be similar to that of the well-known mesostructured silica materials, and the templated structure might not survive the removal of the template. To test whether RF sols could be used to create composite materials that can be pyrolyzed to give mesoporous carbon materials, we examined the use of microemulsion-polymerized polystyrene (PS or cationic microspheres)[21] as a template around which to polymerize RF. This manuscript reports the synthesis of PS/RF mesocomposites and their pyrolysis to yield mesoporous carbon, which has properties analogous to those of carbon aerogels of similar density (~0.7 g cm^{-3}).

Experimental Section

Water was distilled; all other chemicals were used as received from the manufacturer. Gas adsorption data were obtained using a Micromeritics ASAP-2000 porosimeter. BET surface area determinations were performed over a relative pressure range of 0.05−0.16, and 16.2 $Å^2$ was used as the molecular area for nitrogen adsorbed on carbon.[22] Pore size distributions were determined using a variation of the Broekhoff−de Boer method by using Hill's approximation to calculate the thickness of the adsorbed gas layer.[23] Mesopore and micropore volumes were determined from β_s plots; mesopore surface areas were also determined from the β_s plots using $c_{ref} = 2.57$ m^2 cm^{-3}, which corresponds to a molecular area of 16.2 $Å^2$ for N_2.[23] Scanning electron microscopy (SEM) was performed with a JEOL-6300F instrument equipped with a field-emission electron gun operating at an accelerating voltage of 3 kV. Samples were deposited from acetone suspension onto aluminum stubs and sputter-coated with ca. 100 Å of gold−palladium. Transmission electron microscopy (TEM) was performed using a JEOL-2000FX microscope operating at 200 kV. Samples were deposited from an acetone suspension onto Formvar-coated copper grids. Simultaneous thermogravimetric and differential thermal analyses were performed on a Netzsch STA-409 instrument under flowing argon. Resistance measurements were performed using a four-point probe with a digital voltmeter and power supply.[24] Microemulsion-polymerized polystyrene was prepared as previously reported.[25]

Synthesis Using Sodium Carbonate as the Catalyst. Sodium carbonate (0.04 g, 0.4 mmol) was dissolved in water (24 mL) at 70 °C. To this solution were added 35-nm-diameter cetyltrimethylammonium chloride- (CTAC-) coated PS spheres (5 mL, 0.24 M in CTAC, 1.2 mmol) and resorcinol (0.66 g, 6 mmol), followed by formalin (0.9 mL, 12 mmol). After 2 h, a large quantity of purple precipitate had formed. The mixture was stirred at 70 °C for a total of 4.5 h and then filtered. The purple solid was washed with 50 mL of water and dried on the filter (yield 2.40 g). A pellet was pressed from 300 mg of powdered PS/RF using a 13-mm IR pellet die under 10000 lb of pressure. The pellet was carbonized under flowing argon at 2 °C/min to 800 °C followed by a 1-h hold at 800 °C. The pellet was allowed to cool slowly to room temperature. Pellet densities are given in Table 1.

Table 1. Densities of PS/RF Pellets before and after Pyrolysis

sample/ synthesis method[a]	template[b]	ratio[c]	initial density (g cm^{-3})	final density (g cm^{-3})
1A	PS	6	1.06	0.61
2B	PS	6	1.06	0.78
3C	PS	6	1.06	0.62
4D	PS	6	0.80	0.49
5D	PS	4	0.76	0.47
6D	CTAB	5	0.88	0.71
7E	PS	3	1.01	0.78
8F	PS	3	1.01	0.64
9E	PS	3	0.96	0.70
10F	PS	3	0.97	0.79

[a] A, Na_2CO_3 catalysis with template added before condensation of RF; B, A followed by HCl; C, Na_2CO_3 catalysis with template added after condensation of RF; D, HCl catalysis; E, NaOH catalysis; F, NaOH catalysis followed by HCl. [b] PS, polystyrene microspheres; CTAB, cetyltrimethylammonium bromide. [c] Ratio of resorcinol to CTAC.

Synthesis Using Sodium Carbonate as the Catalyst, Acid Treatment. This synthesis was performed as above, except that, after the solid was removed from solution, it was slurried in 50 mL of 0.1 M hydrochloric acid for 24 h at room temperature. The solid was then filtered, washed with water, and dried on the filter.

Synthesis Using Sodium Hydroxide as the Catalyst. A mixture of water (68 mL), CTAC-coated, 37-nm-diameter PS spheres (15 mL, 0.22 M in CTAC, 3.3 mmol), aqueous sodium hydroxide (3.3 mL, 1 M, 3.3 mmol), and resorcinol (1.09 g, 9.9 mmol) was stirred and heated to 90 °C. Formalin (0.7 mL, 9 mmol) was added. After 1 h, a white precipitate formed. After 4 h of stirring at 90 °C, the mixture was poured into a 125-mL polypropylene (PP) bottle and placed in a 90 °C oven. After 12 h in the oven, the mixture was filtered and washed with 120 mL of water. The pink solid was dried on the filter and then oven-dried at 120 °C for 12 h. A pellet (430 mg, 12.8 mm diameter, 3.3 mm thick) was pressed at room temperature using a 13-mm IR pellet die at 10000 lb. The pellet was carbonized by heating under flowing argon to 250 °C over 2 h, holding for 4 h at 250 °C, heating to 800 °C over 5 h, holding for 4 h at 800 °C, and then slowly cooling to room temperature.

Synthesis Using Sodium Hydroxide, Acid Treatment. Composite material was prepared as described above but with the following change. After 12 h in the oven, 1 mL of concentrated HCl was added to the PP bottle, and the mixture was heated to 90 °C for 4 h.

Synthesis in 1 M Hydrochloric Acid. A mixture of water (21.5 mL), a solution of CTAC-coated, 37-nm-diameter polystyrene (PS) spheres (5.0 mL, 0.22 M in CTAC, 1.1 mmol of CTAC), resorcinol (0.73 g, 6.6 mmol), and concentrated hydrochloric acid (2.5 mL, 30 mmol) was heated to 85 °C. Formalin (1.0 mL, 13 mmol) was added, and the mixture was stirred at 85 °C for 16 h, producing a pink precipitate. The solid was removed by vacuum filtration, washed with 50 mL of water, and allowed to dry on the filter. A mixture of 297 mg of this composite and 30 mg of hexamethylenetetramine (HMTA) was pressed into a pellet using a 13-mm-diameter IR pellet die at 10000 lb. The pellet was carbonized by heating under argon to 250 °C over 2 h, holding for 4 h at 250 °C, heating to 800 °C over 5 h, holding for 4 h at 800 °C, and then slowly cooling to room temperature. The pellet was carbonized under argon as described above.

(21) Antonietti, M.; Bremser, W.; Muschenborn, D.; Rosenauer, C.; Schupp, B.; Schmidt, M. *Macromolecules* **1991**, *24*, 6636.
(22) Gregg, S. J.; Sing, K. S. W. *Adsorption, Surface Area, & Porosity*, 2nd ed.; Academic Press: London, 1982.
(23) Lukens, W. W.; Schmidt-Winkel, P.; Zhao, D. Y.; Feng, J. L.; Stucky, G. D. *Langmuir* **1999**, *15*, 5403.
(24) *ASTM F1529-97: Standard Test Method of Sheet Resistance Uniformity Evaluation by In-Line Four-Point Probe with the Dual-Configuration Procedure*; American Society for Testing and Materials: West Conshohocken, PA, 1997.
(25) Lukens, W. W.; Yang, P. D.; Stucky, G. D. *Chem. Mater.* **2001**, *13*, 28.

Table 2. Physical Properties of Carbon Mesocellular Foams (C-MCFs)

sample/ synthesis method[a]	template diameter (nm)	V_{tot}[d] ($cm^3\ g^{-1}$)	V_{mes}[e] ($cm^3\ g^{-1}$)	V_{mic}[f] ($cm^3\ g^{-1}$)	SA_{BET}[g] ($m^2\ g^{-1}$)	SA_{mes}[h] ($m^2\ g^{-1}$)	pore diam[i] (nm)	conductivity ($S\ cm^{-1}$)
1A	35[b]	0.98	0.71	0.10	527	270	31	
2B	35[b]	0.61	0.51	0.12	621	310	21	
3C	35[b]	0.94	0.14	0.00	51	39		
4D	37[b]	1.39	0.43	0.12	641	200	21	
5D	37[b]	1.48	0.38	0.17	632	231	21	
6D	3[c]	0.75	0.00	0.20	475	0		
7E	37[b]	0.62	0.47	0.15	573	240	21	17[j]
8F	37[b]	0.89	0.74	0.17	615	220	41	10[j]
9E	37[b]	0.76						16[j]
10F	37[b]	0.59						19[j]

[a] A, Na_2CO_3 catalysis with template added before condensation of RF; B, A followed by HCl; C, Na_2CO_3 catalysis with template added after condensation of RF; D, HCl catalysis; E, NaOH catalysis; F, NaOH catalysis followed by HCl. [b] Determined by dynamic light scattering. [c] Diameter of a CTAB micelle. [d] Total pore volume determined from the density by assuming a density of 1.5 g cm^{-3} for the carbon skeleton. [e] Volume of mesopores determined from β_s plots. [f] Volume of micropores determined from β_s plots. [g] BET surface area. [h] Mesopore surface area determined from β_s plots. [i] Pore diameter determined using the BdB−FHH method for spherical pores. [j] Four-point probe measurement.

Scheme 1. Synthetic Strategy for Making Mesocellular Carbon Foams

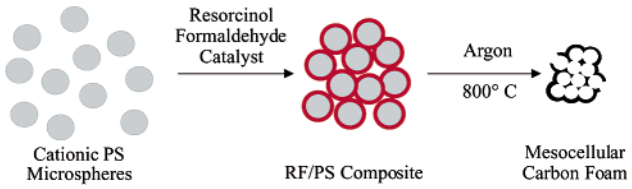

Results

The general synthetic strategy is shown in Scheme 1. Cationic polystyrene microspheres in water are coated with resorcinol/formaldehyde polymer to give a PS/RF composite. Like silica, the RF sol is anionic at high pH and capable of hydrogen bonding at low pH; therefore, conditions that yield PS/silica composites are likely to produce PS/RF composites in which the cationic microspheres act as templates. The composite can then be pyrolyzed to carbonize the RF and depolymerize the PS. Ideally, the product would be a carbon mesocellular foam (C-MCF) in which the pores are templated by the cationic microspheres as in the preparation of silica mesocellular foam (Si-MCF).[25]

Because RF can be prepared both in acidic and alkaline solution using a variety of catalysts,[26] different approaches to the preparation of RF sols and PS/RF composites were examined. The structures of the C-MCFs resulting from the different syntheses provide insight into the formation of the PS/RF composites. The PS/RF composites were compressed into 13-mm-diameter pellets and pyrolyzed at 800 °C under argon to yield C-MCFs, the physical properties of which are given in Tables 1 and 2.

The presence of the template in the PS/RF composite can be inferred from the weight losses of the samples upon pyrolysis. All of the samples, except 6, lose 80−85% of their mass upon pyrolysis. Sample 6, which does not contain PS microspheres but does contain surfactant, loses only 70% of its mass. In comparison, RF loses only about 50% of its mass upon pyrolysis.[27] Furthermore, thermogravimetric analysis of the PS/RF composites under argon (Figure 1) shows a large endothermic loss of mass at 400 °C, which is consistent with depolymerization of PS.[28]

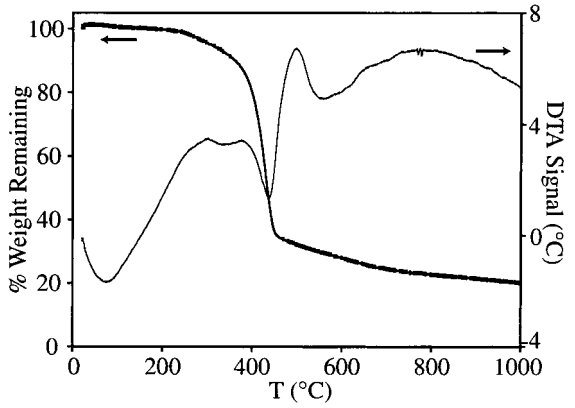

Figure 1. TGA/DTA scan of a polystyrene microsphere/ resorcinol/formaldehyde composite showing large endothermic loss of mass at 400 °C.

Additional information about the structure of the C-MCFs can be gained by examining the nitrogen adsorption isotherms, which are shown in Figure 2 along with the pore size distributions derived from the adsorption branch of the isotherms. As is evident from Figure 2 and Table 2, samples synthesized using PS templates produce mesoporous materials with mesopores that are roughly two-thirds the size of the templates. The exception is sample 3, which was made by preparing the RF sol before adding the template. This ratio is in good agreement with the overall shrinkage of the pellets upon carbonization. The dimensions of the pyrolyzed pellets are all roughly two-thirds of their initial dimensions. The agreement between the shrinkage of the pores and the pellets is consistent with congruent shrinking of the pellets after loss of the template.

In addition to mesopores, all of the samples, except sample 3, contain micropores. The micropore volumes of the samples can be obtained from a modified standard adsorption plot (β_s plot),[23] as shown in Figure 3. The micropore volumes of the samples, shown in Table 2, vary from 0.1 to 0.2 $cm^3\ g^{-1}$. The presence of micropores

(26) Knop, A.; Scheib, W. *Chemistry and Applications of Phenolic Resins*; Springer-Verlag: New York, 1979.

(27) Even, W. R.; Crocker, R. W.; Hunter, M. C.; Yang, N. C.; Headley, T. J. *J. Non-Cryst. Solids* **1995**, *186*, 191.

(28) Westerhout, R. W. J.; Waanders, J.; Kuipers, J. A. M.; van Swaaij, W. P. M. *Ind. Eng. Chem. Res.* **1997**, *36*, 1955.

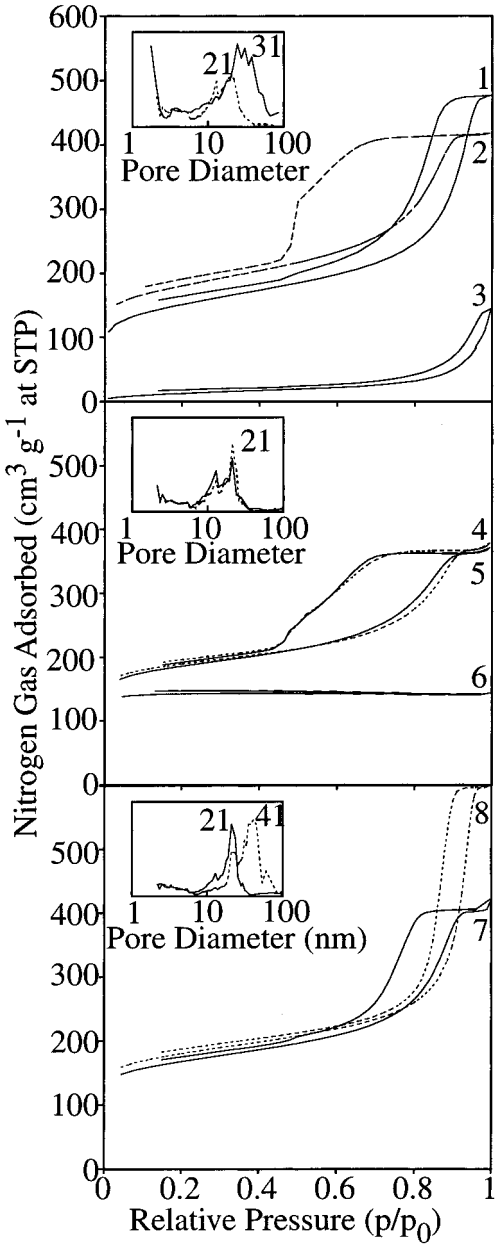

Figure 2. Nitrogen adsorption isotherms and BdB−FHH pore size distributions (inset) for carbon mesocellular foams. The isotherms are labeled according to the sample number in the text.

renders the BET surface area largely meaningless as micropores adsorb large volumes of gas at low pressures, producing a BET surface area that overestimates the actual surface area of the material.[29] However, the surface area of the mesopores can also be determined from the β_s plot. The surface area of the mesopores varies from 200 to 300 m^2 g^{-1}. For sample 3, the only sample without micropores, the BET surface area of 51 m^2 g^{-1} is in good agreement with the total surface area of 53 m^2 g^{-1} determined from the β_s plot. Like the surface area of the mesopores, the volume of the mesopores varies only slightly among the samples from 0.4 to 0.7 cm^3 g^{-1}. The micropore and mesopore volumes and the mesopore surface areas do not vary systematically when the synthesis conditions are changed.

(29) Schneider, P. *Appl. Catal. A: Gen.* **1995**, *129*, 157.

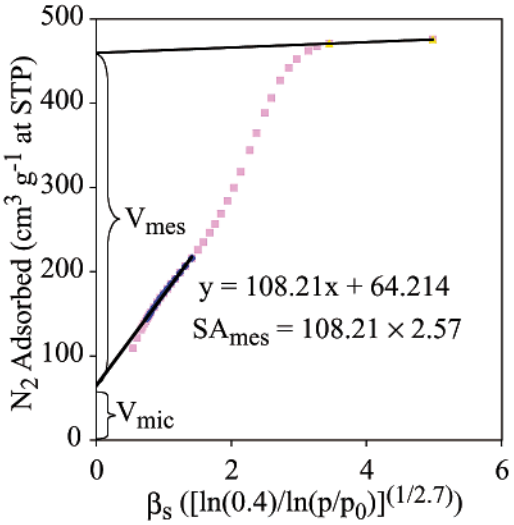

Figure 3. Modified standard adsorption plot of a carbon mesocellular foam (sample 8) showing V_{mic}, V_{mes}, and SA_{mes}.

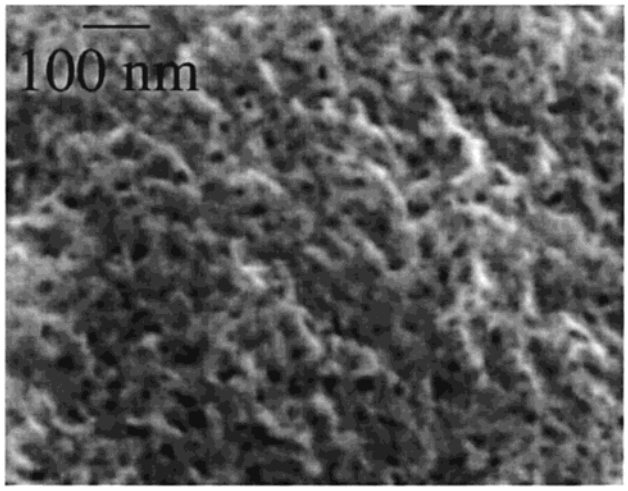

Figure 4. SEM image of a carbon mesocellular foam showing the ~20-nm pores.

The volume of macropores in the samples does vary widely. For samples 3−6, the macropore volume, determined from the total pore volume and the micropore and mesopore volumes, varies from 0.5 to 0.9 cm^3 g^{-1}, whereas the other samples are not appreciable macroporous. The large macropore volumes result from the use of hexamethylenetetramine (HMTA) to cross-link the RF in samples 4−6 during pyrolysis.[26] These pellets consisted of 10% HMTA and 90% PS/RF by weight prior to pyrolysis. The HMTA vaporizes during pyrolysis, producing additional macropores. The origin of the macropores in sample 3 is discussed below. Apart from the larger macropore volumes, samples 4 and 5 closely resemble the other C-MCF samples.

The mesopores in the C-MCFs can be directly observed using scanning electron microscopy as shown in Figure 4. However, the mesopores are not readily apparent in TEM images, as shown in Figure 5. None of the C-MCF particles examined by TEM was thin enough to obtain an image through the bulk of the sample, which would show the mesopores. However, the TEM images clearly reveal the basic structure of the C-MCF, which is quite different from that of the analogous siliceous materials. The C-MCF material is

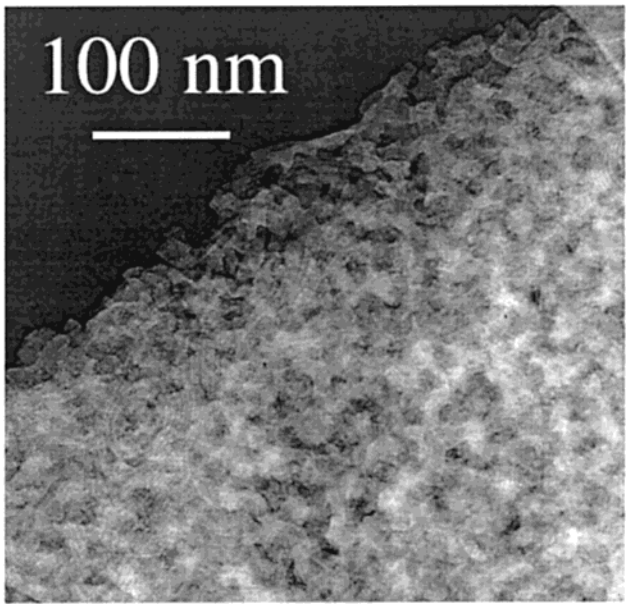

Figure 5. TEM image of a carbon mesocellular foam showing the ~10-nm-diameter nodes that comprise the carbon skeleton.

composed of small, ~10 nm, beads of carbon linked into a matrix through wide necks. This structure is very similar to that reported for carbon aerogels.[30,31]

The final column of Table 2 shows the electrical conductivities of the C-MCF samples. The conductivities vary with the density of the C-MCFs. As is the case for carbon aerogels, the denser C-MCFs have greater electrical conductivities.[32] However, because of the narrow range of densities examined, a quantitative relationship between the conductivity and the density cannot be determined with any precision.

Discussion

These C-MCF materials are strongly reminiscent of carbon aerogels with similar densities. The two types of materials have similar conductivities, and the skeletal structures of the two materials consist of linked spheres of carbon. In addition, the BET surface areas of C-MCFs are similar to those of carbon aerogels of similar densities, and in both materials, the surface area of the mesopores comprises roughly half of the total surface area determined by the BET method.[33] These similarities are hardly surprising as both materials are synthesized by preparing RF sols in aqueous solution and pyrolyzing the RF network into a carbon skeleton. The major difference between these materials is the origin of the pores. In the C-MCFs, the pores are clearly templated by the PS spheres, which depolymerize during carbonization of the PS/RF composite materials. The role of the PS spheres as templates is illustrated by the fact that samples prepared with surfactants but without the PS spheres do not possess mesopores. However, the mechanism of assembly of PS and RF to form the PS/RF composites must be addressed.

Scheme 2. Proposed Mechanism for the Formation of PS-Templated Carbon Foams

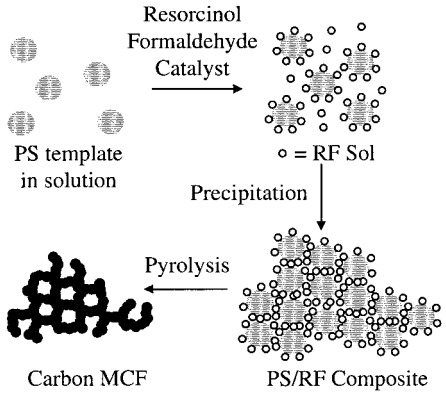

The most surprising result of the synthetic studies is the lack of systematic changes in the structure of the C-MCF materials in response to different synthetic conditions. Apart from the decreased density and increased macroporosity of the pellets containing 10 wt % HMTA, the densities, pore volumes, and mesopore surface areas of the samples are very similar, with the exception of samples 3 and 6. This similarity suggests that the templating mechanism is the same, or very similar, for all of the samples. The interesting exception is sample 3, which was synthesized by forming the RF sol prior to adding the template. In all other cases, the PS template was added before forming the RF sol. This situation is in marked contrast to the preparation of Si-MCFs, which have structures that vary strongly with different synthetic conditions.[25]

A templating mechanism that is consistent with the data and the known chemistry of RF is shown in Scheme 2.[26,31] In this mechanism, the RF polymerizes until the sol reaches a certain size (~10 nm from TEM). At this point, the RF sol forms an insoluble agglomerate with the PS microspheres. The composite precipitates, halting the further growth of the RF particles in the composite. The RF sol particles that remain in solution can continue to grow but do not precipitate.

This mechanism is very similar to that described for the early stages of the formation of RF gels. In addition, it explains the lack of mesoporosity in sample 3. Because no template was present during the synthesis of the RF sol, the particles were able to grow much larger than in the other syntheses without precipitating. Addition of the PS template produced a composite material that contained the template as determined by the weight loss upon pyrolysis; however, the RF particles were much larger than the template. Consequently, the porosity of the resulting carbon was only "textural mesoporosity"[34] consisting of the space between the large RF sol particles.

Although the C-MCF materials and carbon aerogels have some similarities, a number of differences exist between these materials. The carbon aerogel synthesis is more easily tuned than the C-MCF synthesis. Carbon aerogels can by prepared with densities ranging from 0.1 to 1.1 g cm^{-3}.[11,30] In comparison, the densities of C-MCF materials fall into the narrow range of 0.5−0.8 g cm^{-3}. Attempted syntheses of C-MCFs with lower

(30) Pekala, R. W.; Schaefer, D. W. *Macromolecules* **1993**, *26*, 5487.
(31) Pekala, R. W. *J. Mater. Sci.* **1989**, *24*, 3221.
(32) Lu, X. P.; Nilsson, O.; Fricke, J.; Pekala, R. W. *J. Appl. Phys.* **1993**, *73*, 581.
(33) Hanzawa, Y.; Kaneko, K.; Pekala, R. W.; Dresselhaus, M. S. *Langmuir* **1996**, *12*, 6167.
(34) Tanev, P. T.; Pinnavaia, T. J. *Science* **1995**, *267*, 865.

densities by using a smaller ratio of resorcinol and formaldehyde to CTAB surfactant did not produce C-MCFs with lower densities. Instead, these conditions produced smaller C-MCF pellets with densities and pore structures similar to those of the C-MCFs reported above. In addition, the pore size in carbon aerogels can by changed by varying the synthetic conditions.[35] These differences result from the different syntheses. Because carbon aerogels are formed by pyrolyzing RF aerogels that have variable densities, mesoporous carbon materials can be readily synthesized with different properties. The agglomeration templating mechanism of formation of the C-MCF materials requires the synthesis of different templates to change the properties of the porous carbon as the properties of the porous carbon material do not change greatly with synthetic conditions.

One other difference is the duration of the synthesis. The synthesis of C-MCFs is much faster than the synthesis of carbon aerogel. The major reason for the faster synthesis of C-MCFs is the fact that the RF sols do not need to gel; the template and RF sol simply agglomerate and precipitate. In addition, the solvent-exchange and supercritical-extraction steps are not needed to make C-MCFs as the template is lost during pyrolysis.

A final difference is the nature of the precursor to the carbon material. In C-MCF materials, the precursor is a nonporous, PS/RF composite powder that can be pressed into shapes (cylindrical shapes, at least). The pellets pressed from the composite pellets are not fragile largely because they are nonporous.

(35) Tamon, H.; Ishizaka, H.; Araki, T.; Okazaki, M. *Carbon* **1998**, *36*, 1257.

Conclusion

Carbon mesocellular foams can be synthesized by templating a resorcinol/formaldehyde sol with microemulsion-polymerized polystyrene to prepare PS/RF composites. These composite materials can be formed by several different synthetic routes. Pyrolysis of the PS/RF composite depolymerizes the template and forms the carbon skeleton of the C-MCF in the same process. The resulting C-MCFs are similar to carbon aerogels of similar densities, $\sim$0.7 g cm^{-3}. The templating mechanism is believed to proceed by agglomeration of RF sols with the template. The agglomerated composite material then precipitates from solution, halting the further growth of the RF sol particles. The precipitate can be filtered, dried, and pressed into pellets. The pyrolyzed pellets have large mesopore volumes, considerable microporosity, and good electrical conductivity. The C-MCF synthesis does not afford the fine control over density and pore structure offered by carbon aerogel synthesis, but the C-MCF synthesis does enable the rapid synthesis of mesoporous carbon with good electrical conductivity.

Acknowledgment. This work was supported by the NSF under Grants DMR-9520971 and DMR-9634396 and the U.S. Army Research Office under Grant DAAH04-96-2-0443. We thank Prof. David Pine for the use of the light-scattering goniometer. W.L. is grateful to the National Science Foundation for a Postdoctoral Fellowship. We made use of the UCSB Materials Research Laboratory Central Facilities supported by the NSF under Award DMR-9632716.

CM010904Z